Supplementary materials

A high performance thermal expansion offset composite cathode for IT-SOFCs

Kang Liu[1,2], Fei Lu[1,2], Xusheng Jia[1,2], Hao He[1], Jinrui Su[1], and Bin Cai[1,2]*

[1] Key Laboratory of Material Physics, Ministry of Education, School of Physics and Microelectronics, Zhengzhou University, Zhengzhou 450052, China
[2] Institute of Intelligent Sensing, Zhengzhou University, Zhengzhou 450001, China

*Corresponding author: Prof. Dr. Bin Cai (B. Cai), bcai@zzu.edu.cn (OCRID: 0000-0002-8587-0181)

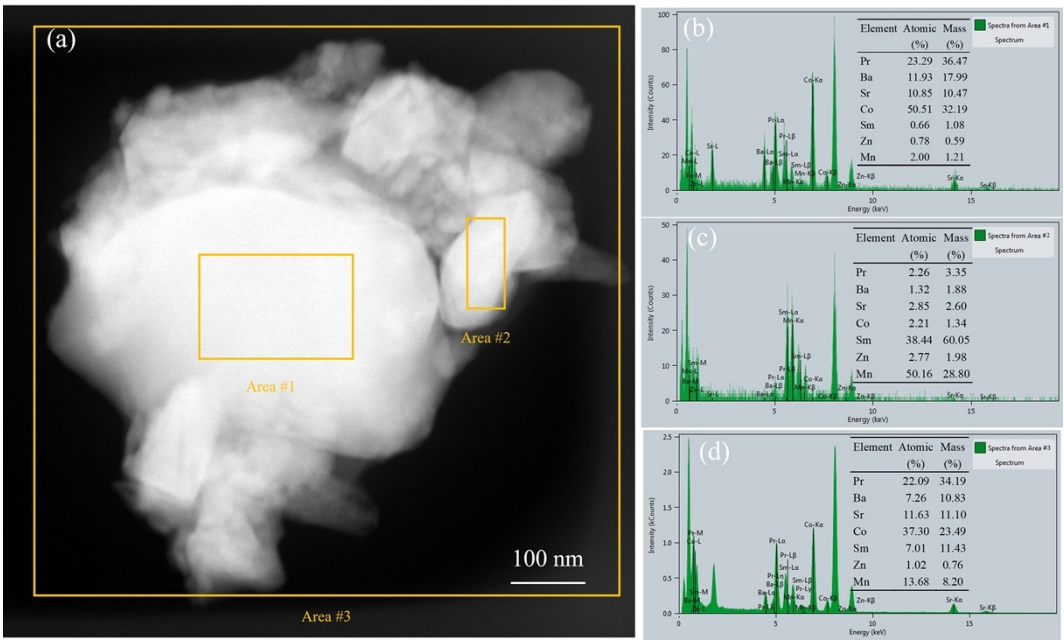

Fig. S1 STEM micrograph of PBSC-SZM (a), EDS scanning results of area #1 (b), area #2 (c) and area #3 (d).

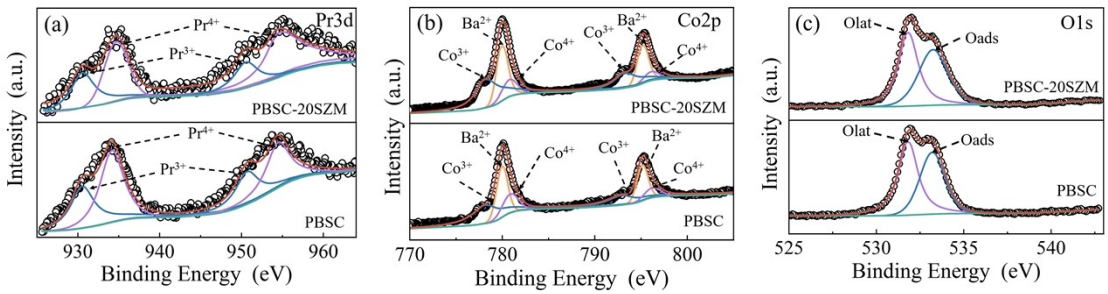

Fig. S2 XPS spectra of (a) Pr3d, (b) Ba3d and Co2p, and (c) O1s for both PBSC-20SZM and PBSC.

Table S1 Fitted binding energy and ratio of Pr, Co, Ba and O with different status.

Element		PBSC			PBSC-20SZM		
		Binding energy (eV)		at.%	Binding energy (eV)		at.%
		Pr and Ba $3d_{3/2}$, $Co2p_{1/2}$, O1s	Pr and Ba $3d_{5/2}$, $Co2p_{3/2}$		Pr and Ba $3d_{3/2}$, Co $2p_{1/2}$, O1s	Pr and Ba $3d_{5/2}$, Co $2p_{3/2}$	
Pr	Pr^{3+}	949.8	929.5	48.65	949.9	929.6	48.48
	Pr^{4+}	954.2	933.6	51.35	954.4	933.9	51.52
Ba	Ba^{2+}	795.1	780.1	-	795.1	780.1	-
Co	Co^{3+}	793.1	778.1	76.91	792.8	778.8	77.74
	Co^{4+}	796.1	780.8	23.09	796.2	780.9	22.26
O	O_{lat}	531.8	-	70.29	531.7	-	70.97
	O_{ads}	533.3	-	29.71	533.2	-	29.03

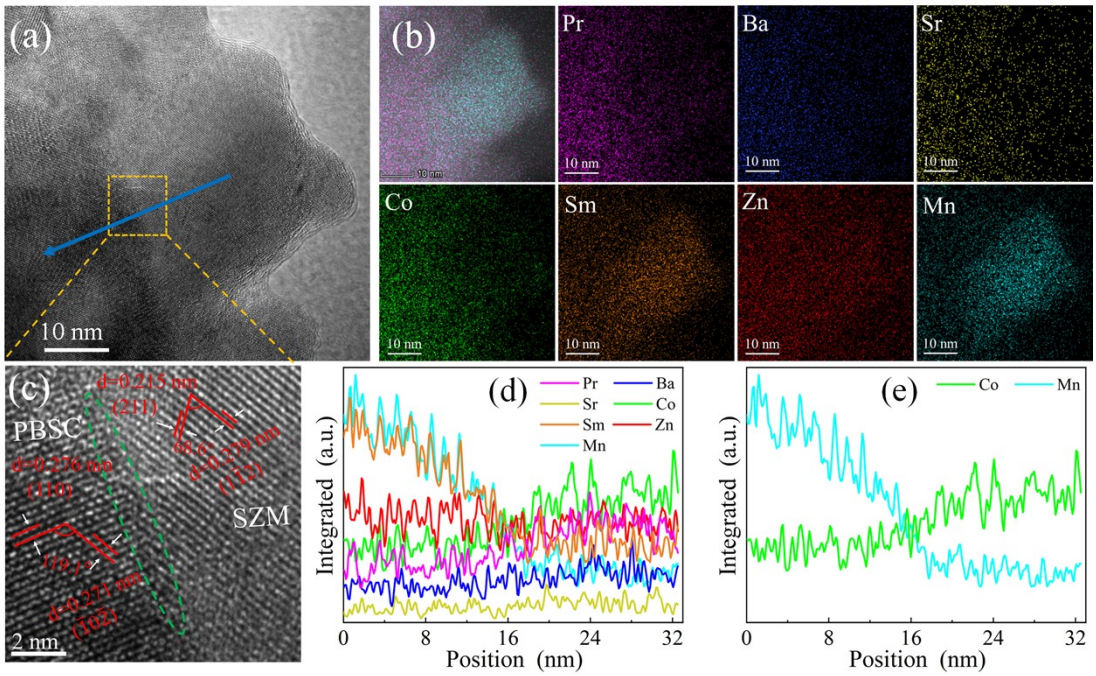

Fig. S3 HRTEM image of PBSC-SZM powder (a), corresponding EDS-mapping (b), lattice fringe image PBSC-SZM (c) of region shown in (a), the relative content of all metal elements (d) and only Co and Mn (e) as a function of position by EDS line scanning of blue arrow shown in (a).

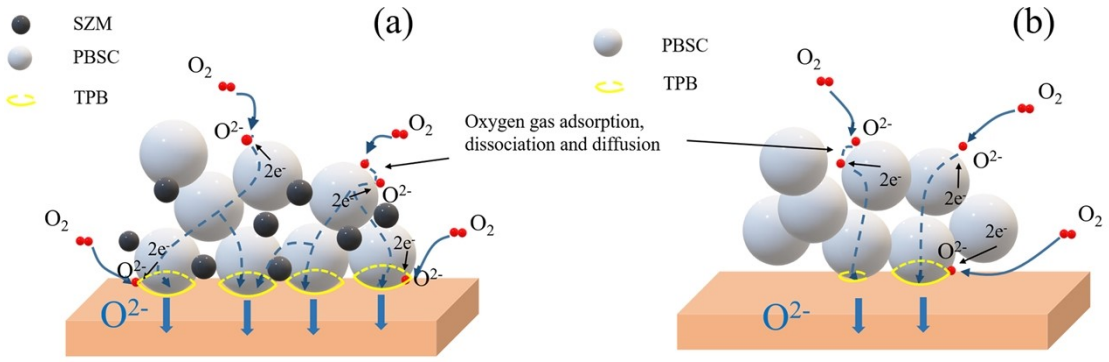

Fig. S4 Schematic illustration on the effect of SZM addition in PBSC cathode on the transportation channels and TPB length. (a) PBSC-20SZM and (b) PBSC cathodes.

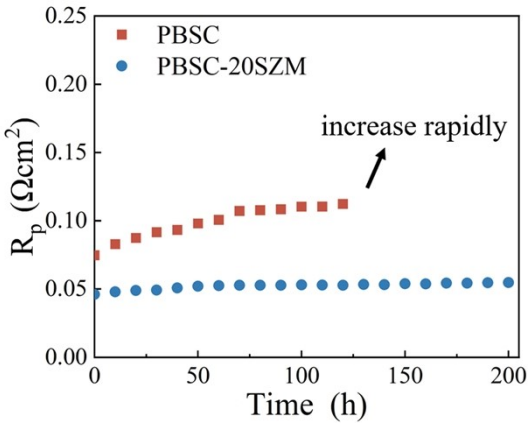

Fig. S5 Polarization resistance R_p as a function of working time for single cells with PBSC and PBSC-20SZM cathodes.

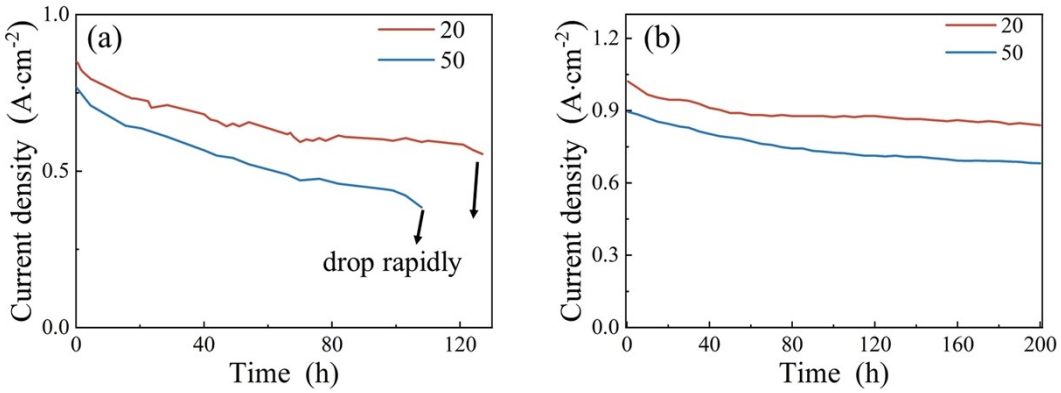

Fig. S6 Effects of cathode thicknesses (20 and 50 μm) on long-term stability of single cells with (a) PBSC and (b) PBSC-20SZM cathodes tested at a constant cell voltage of 0.7 V and 873 K.

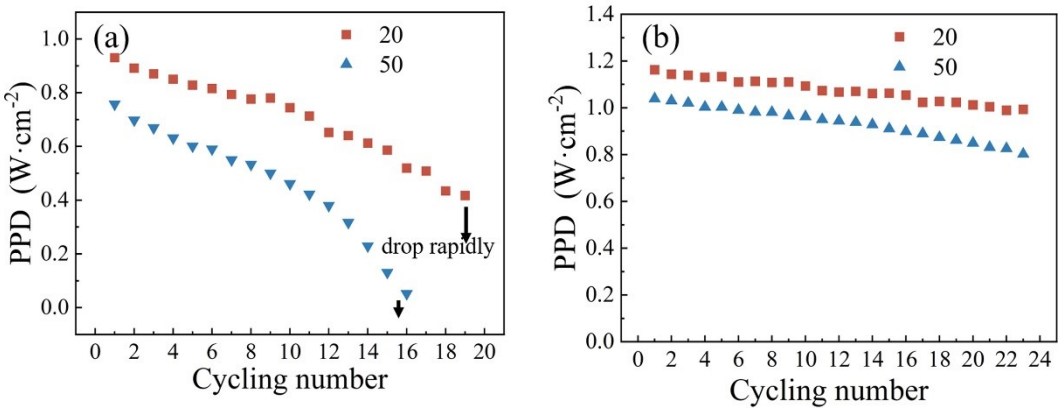

Fig. S7 Effects of cathode thicknesses (20 and 50 μm) on performance of single cells with (a) PBSC and (b) PBSC-20SZM during thermal cycling between 723 and 873 K with heating and cooling rates of 10 K min^{-1}. Output PPD was recorded at 873 K.

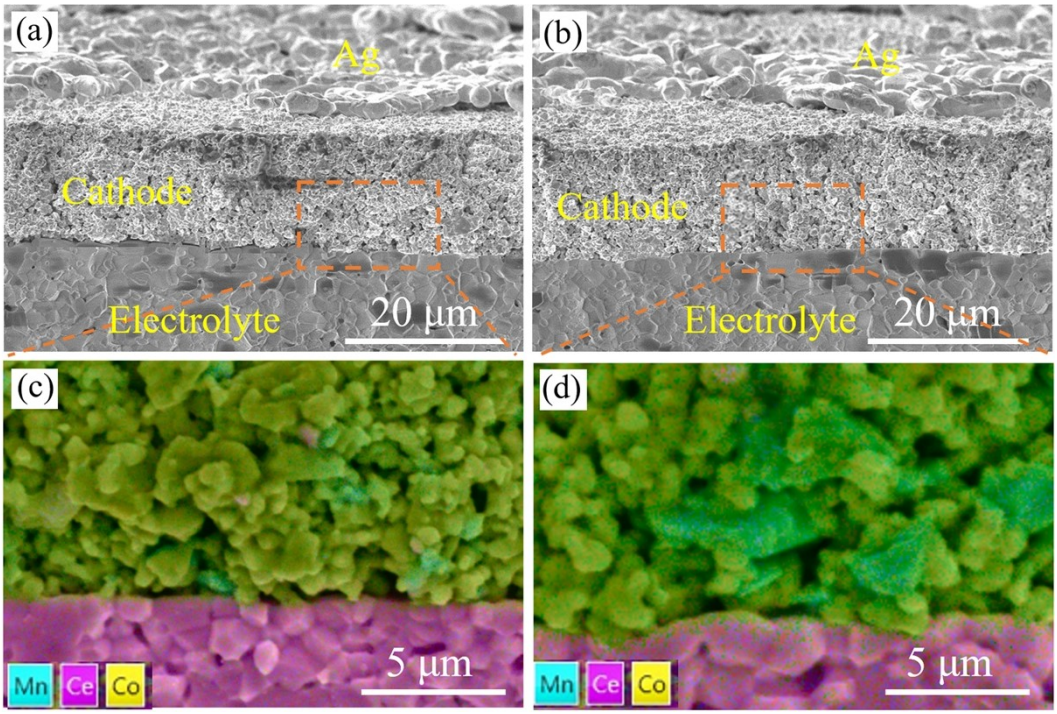

Fig. S8 Cross-sectional SEM micrographs and local area EDS mapping of single cells with PBSC-10SZM (a and c) and PBSC-30SZM (b and d) tested for 5 h at 0.7 V and 873 K.

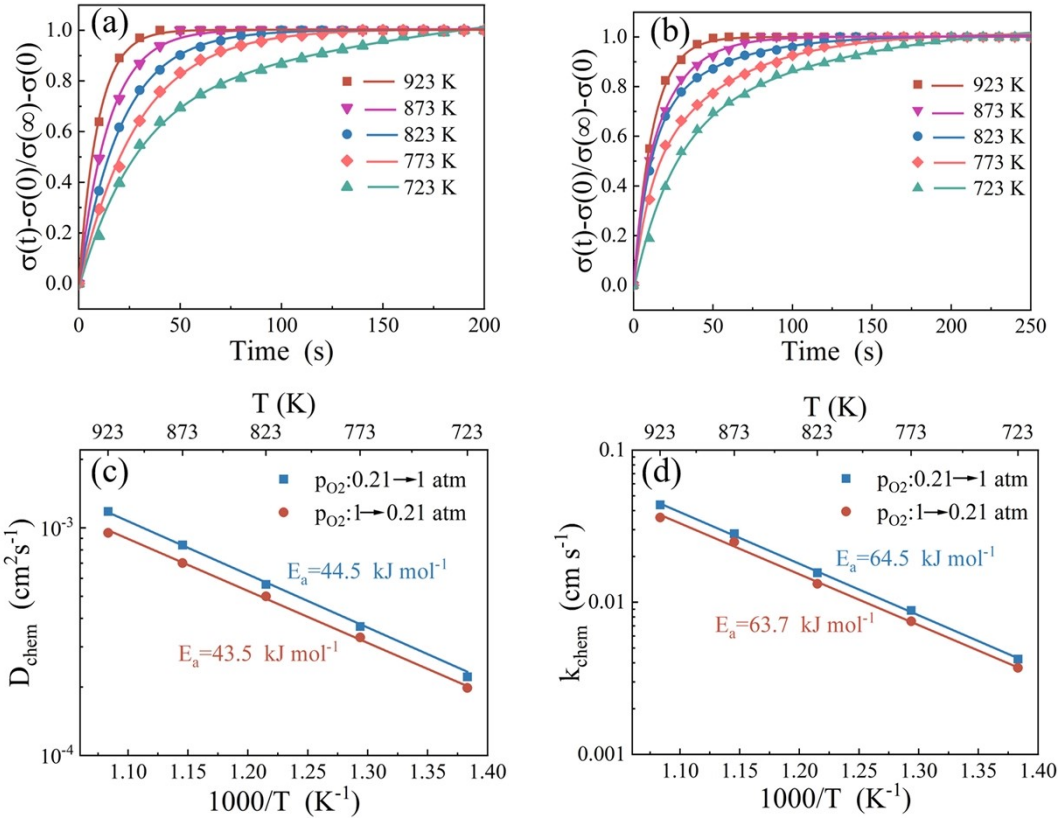

Fig. S9 ECR responses curves of PBSC at various temperatures after an abrupt change in the oxygen partial pressure from 0.21 to 1 atm (a) and its reduction step (b). Arrhenius plots of D_{chem} (c) and k_{chem} (d) of PBSC oxides from ECR method.

Table S2 D_{chem} and k_{chem} data of PBSC and PBSC-20SZM at 723-923 K.

T (K)	Sample	oxidation step		reduction step	
		D_{chem} (10^{-4} cm^2 s^{-1})	k_{chem} (10^{-3} cm s^{-1})	D_{chem} (10^{-4} cm^2 s^{-1})	k_{chem} (10^{-3} cm s^{-1})
723	PBSC	2.21	4.23	1.99	3.74
	PBSC-20SZM	1.15	3.10	0.926	2.55
773	PBSC	3.68	7.83	3.36	7.54
	PBSC-20SZM	1.49	5.17	1.27	4.37
823	PBSC	5.64	14.6	5.08	13.2
	PBSC-20SZM	2.28	8.08	1.98	7.16
873	PBSC	7.41	22.2	6.17	23.8
	PBSC-20SZM	2.99	15.5	2.07	10.1
923	PBSC	11.5	43.7	9.55	36.2
	PBSC-20SZM	5.15	24.1	4.05	19.3